

Non-Sparse Phantom for Compressed Sensing MRI Reconstruction

D. S. Smith¹, and E. B. Welch¹

¹Radiology and Radiological Sciences and Institute of Imaging Science, Vanderbilt University, Nashville, TN, United States

INTRODUCTION Compressed sensing (CS) MRI (1), a growing application of compressed sensing (2,3), is experiencing a period of rapid technique development. The ubiquitous Shepp-Logan phantom often serves as the de facto standard for reconstruction accuracy. The advantages to the Shepp-Logan phantom are the standard construction, the absence of noise, the sparsity of its gradient image, and roughly anatomical shape. CS MRI reconstruction typically works by minimizing the L1 norm of the gradient, or total variation (TV) of the reconstructed image. Because the Shepp-Logan phantom is extremely sparse under a gradient transform, most CS algorithms can exactly reconstruct it from very few Fourier samples. Real anatomical images, however, are not piecewise constant and are not sparse under a gradient transformation. Therefore, CS MRI reconstructions of more realistic images are not exact reconstructions, but rather parameter-dependent optima. Typically this means the resulting image is a compromise between loss of fine detail and elimination of ghosting artifacts. This balance between spatial resolution and artifacts is not well understood, and the Shepp-Logan phantom does not provide features amenable for studying the trade-off. Additionally, real anatomical images are not an ideal test case for CS MRI reconstruction because all real images contain noise, which sets an upper bound on reconstruction accuracy. This will become increasingly important as CS MRI moves toward non-convex optimization paradigms (4), which seem to be superior to L1 minimization. We have, to support CS algorithm development, designed a phantom image that is not sparse under a gradient transformation, is noiseless, and contains features known to be difficult to reconstruct under a TV-L1 minimization CS MRI reconstruction.

MATERIALS AND METHODS The phantom image consists of four quadrants, numbered from upper right, counterclockwise to lower right, as with the Cartesian plane. Quadrant I contains low-contrast squares and a large linear-intensity “island.” Quadrant II contains sixteen low-contrast disks of varying radii. Quadrant III contains a large quadratic “hole” and four smaller Gaussian “bumps.” Quadrant IV contains vertical and horizontal line pairs and concentric circles with a range of spacings. These will cause ghosting if high spatial frequencies are omitted from the Fourier data. The MATLAB (Natick, MA) code for our phantom may be freely downloaded (5). A CS MRI scan was simulated by creating a 256 x 256 instance of each phantom and then randomly discarding 85% of the columns of the Fourier transform of each image with the sampling density distributed as k^{-1} . The same columns were discarded for both images. Images were then reconstructed using a split Bregman (6) TV-L1 minimization algorithm.

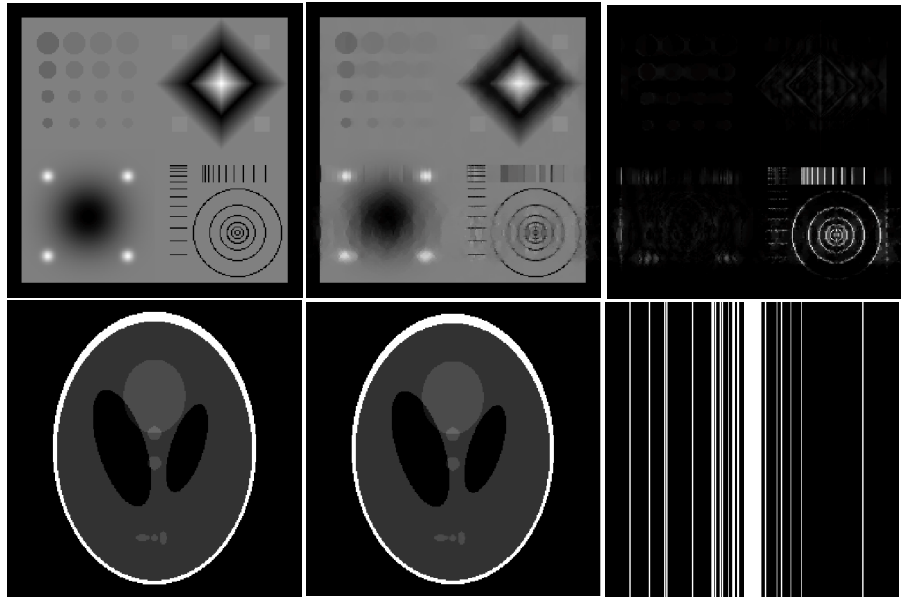


Figure 1: CS reconstructions of our proposed phantom and the Shepp-Logan phantom at 15% sampled. The original CS phantom (upper left), the reconstructed CS phantom (upper middle), and the difference (upper right). The original Shepp-Logan (lower left) was recovered exactly (lower middle). The mask used (lower right) is shown for reference.

RESULTS Fig. 1 shows the results of the CS reconstruction and the data mask used. The reconstruction was least accurate in recovering high frequency features in the horizontal direction and in maintaining contrast of the low-contrast disks and squares. The ghosting due lack of high-frequency information also affected other objects in the reconstruction. For example, the borders of the Gaussian bumps in Quadrant IV are lost. This could have implications, for example, in detection of enhancing tumors using CS-accelerated MRI techniques. For comparison, both Shepp-Logan phantom images are shown, but the reconstruction accuracy was almost exact. Table 1 shows the sparsity of each phantom under a TV transformation and the normalized mean square error (NMSE) of the reconstruction. Our proposed phantom is significantly less sparse and produces a much higher NMSE in the CS reconstruction.

DISCUSSION We have demonstrated the differences in a simple CS MRI reconstruction applied to both our proposed CS phantom and the traditional Shepp-Logan phantom. It is our hope that this image will motivate development of better tools for studying the accuracy of CS solvers, the properties of CS reconstruction artifacts (especially in medical imaging), and the noise properties of CS MRI with and without measurement error.

REFERENCES [1] Lustig et al.; *Mag Reson Med* 2007;58:1182-1195, [2] Candes et al.; *IEEE Trans Inf Theory* 2006;52:489-509, [3] Donoho, D.; *IEEE Trans Inf Theory* 2006;52:1289-1306, [4] Trzasko, J. and Manduca, A.; *IEEE Trans. Med. Imag.* 2009;28:106-121, [5] <http://vuuis.vanderbilt.edu/~dss/csphantom/>, [5] Goldstein, T., and Osher, S.; *SIAM J Imag Sci* 2009;2:323-343

ACKNOWLEDGEMENTS NIBIB T32 EB001628

	Sparsity	Reconstruction NMSE
Shepp-Logan	0.0333	1.29E-04
This Work	0.362	0.380

Table 1: TV sparsity and normalized mean square error (NMSE) for our proposed phantom and the Shepp-Logan phantom.